The novel disc-like molecule $[Mn_{19}O_{12}(moe)_{14}(moeH)_{10}]\cdot MOEH$ ($MOE = OC_2H_2OCH_3$) can be prepared by metathesis from $MnCl_2$ and potassium methoxyethoxide, and its solid-state structure has been determined by single-crystal X-ray diffraction.

It is one of the largest alkoxide molecules as well as one of very few Mn alkoxides reported. The solubility and reactivity, together with the layer structure, make it a very good precursor for Mn-containing ceramics based on MnO_x layers.

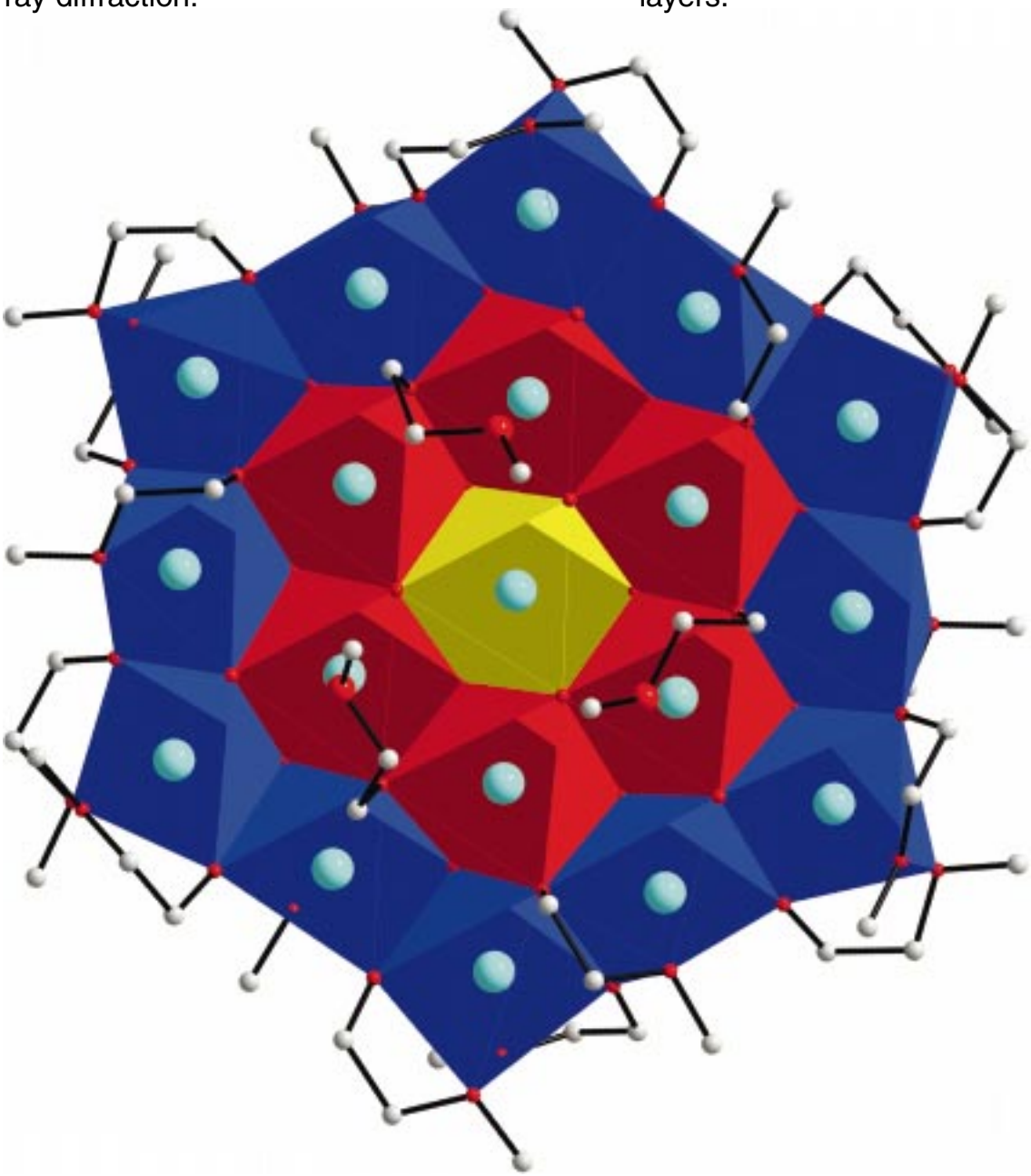

For more information see the following pages.

0947-6539/01/0716-3438 $ 17.50+.50/0 *Chem. Eur. J.* **2001**, *7*, No. 16

Preparation, Structure, and Properties of a New Giant Manganese Oxo-Alkoxide Wheel, $[Mn_{19}O_{12}(OC_2H_4OCH_3)_{14}(HOC_2H_4OCH_3)_{10}] \cdot HOC_2H_4OCH_3$

I. Annika M. Pohl,[a] L. Gunnar Westin,*[a] and Mikael Kritikos[b]

Abstract: Alkoxides are of great interest as precursors for sol-gel processing of advanced ceramic materials, but there is very little general knowledge about the low-valent 3d-element alkoxides. The novel oxo-alkoxide, $[Mn_{19}O_{12}(moe)_{14}(moeH)_{10}] \cdot MOEH$ ($MOE = OC_2H_2OCH_3$), was prepared, by metathesis and auto-decomposition, from $MnCl_2$ and potassium methoxyethoxide in toluene/MOEH, and the solid-state structure was determined from single-crystal X-ray diffraction data: trigonal cell, space group $R\bar{3}$ (no. 148), $a = 27.560(3)$, $c = 19.294(2)$ Å, $Z = 3$, $R1 = 0.0737$, $wR2 = 0.1609$. The individual molecules are shaped as flat discs and all Mn atoms are divalent and octahedrally coordinated by oxygen atoms in a CdI_2-type layer structure. The central Mn atom is coordinated by six μ_3-oxo atoms, the six middle ring Mn-atoms by two μ_3-oxo atoms and four MOE(H) groups, while the peripheral ring contains twelve Mn atoms coordinated by one μ_3-oxo atom and five MOE(H) groups. Differential scanning calorimetry studies showed that the first and irreversible changes start at about 100 °C. The continuous decrease of $\chi_M T$ with decreasing temperature below 150 K in the magnetic susceptibility measurements is probably due to antiferromagnetic interactions. FTIR and UV/Vis spectroscopy of solid and dissolved samples showed that the solid-state structure changes at least to some extent on dissolution in toluene/MOEH.

Keywords: alkoxides · IR spectroscopy · manganese · structural elucidation · UV/Vis spectroscopy

Introduction

Alkoxides are the most popular precursors for the sol-gel processing of complex high-tech ceramics in the forms of thin films and nanophase powders. Their popularity stems from the extensive possibilities of adjusting the properties by varying the alkyl parts of the alkoxo groups and from the possibility of introducing two or more different types of metal ions into the same molecule through sharing of alkoxo bridges. Thereby, heterometallic precursors are obtained that provide an atomic-scale mixing of the constituent metallic elements. The extreme homogeneity of the metal composition is valuable when the target ceramic materials are prepared at low temperatures; this reduces the loss of volatile oxides, prevents unwanted reactions with film substrates and permits one to obtain metastable amorphous or crystalline oxides.

[a] Associate Professor L. G. Westin, I. A. M. Pohl
Department of Inorganic Chemistry, Ångström Laboratory
Uppsala University, 75121 Uppsala (Sweden)
Fax: (+46) 18-513-548
E-mail: gunnar.westin@kemi.uu.se

[b] Associate Professor M. Kritikos
Department of Structural Chemistry, Arrhenius Laboratory
Stockholm University, 10691 Stockholm (Sweden)

Many functional ceramics contain low-valent 3d elements, but comparatively few studies have been conducted on alkoxide precursors for these materials, even for the homometallic alkoxides, and reliable high-yield synthetic routes and structural data are very rare. Instead, mixtures of alkoxides and 3d-element salts are normally used as precursors; this limits the possibility to control the particle size, crystallisation and oxidation state of the ceramics, and normally increases the preparation temperatures.

Manganese-containing materials have received much interest lately, and a wide span of applications are in actual or intended use. Perhaps the most rapidly growing interest has been devoted to the preparation and studies of $La_{0.67}Ca_{0.33}MnO_3$ and its derivatives; this is due to the fact that the highest Colossal Magnetic Resistance (CMR) effects known today are found in these compounds.[1–3] Other manganese-containing ceramics have also proved interesting from a CMR point of view, for example, $(La,Sr)MnO_3$[4, 5] and $Tl_2Mn_2O_7$.[6, 7] A large number of simple or complex oxides, such as Mn oxides, Mn-substituted perovskites and barium hexaaluminates are of interest as various types of catalysts,[8] and the spinel $LiMn_2O_4$ is being investigated as a cathode material in high-performance batteries.[9] The compound *hex*-$YMnO_3$ has attracted attention as a candidate for magnetic data storage

  0947-6539/01/0716-3439 $ 17.50+.50/0

with less severe fatigue problems than the presently used piezoelectric transducer (PZT).[10–13] A large variety of manganese spinels with designed hard or soft magnetic properties are already used in many applications.[14]

The manganese alkoxides form one of the least studied alkoxide systems. Only a few synthetic routes have been reported, and some of them are questionable, since the materials are reported as dark brown or black viscous liquids, which indicates extensive oxidation. Almost all of the divalent manganese alkoxides are insoluble polymers, for example, $[\{Mn(OMe)_2\}_n]$, $[\{Mn(OEt)_2\}_n]$ and $[\{Mn(OiPr)_2\}_n]$, or are soluble only with the aid of bulky alkoxo groups and adducts that contain strong donors, for example, pyridine and tetrahydrofuran.[15, 16] For alkoxo groups that solely contain hydrocarbon radicals, only very large R groups result in soluble compounds, for example, $R = OCH(iPr)_2$.[17] The structures of some heterometallic alkoxides containing manganese are known: $[Ge_2Mn(OtBu)_6]$,[18] $[Mn_2Sn_2(OtBu)_8]$,[18] $[Mn_2Sb_4(OEt)_{16}]$,[19] $[Mn_7Sb_4O_4(OEt)_{18}(HOEt)_2]$[20] and $[Mn_8Sb_4O_4(OEt)_{20}]$.[21]

In the search for a soluble Mn alkoxide for sol-gel processing, we found that the manganese methoxyethoxide has a high solubility in suitable organic solvents such as toluene/MOEH ($MOE = OC_2H_5OCH_3$). After crystallisation and structure determination, the alkoxide turned out to have the composition $[Mn_{19}O_{12}(moe)_{14}(moeH)_{10}] \cdot MOEH$. To our knowledge, this is the largest molecular methoxyethoxide reported. The number of structurally determined methoxyethoxides is small, but a few other divalent compounds have been reported: $[Pb(moe)_2]_n$, which consists of linear chains,[22] and $[Ca_9(moe)_{18}(moeH)_2]$, which consists of nonanuclear molecules in a coplanar CdI_2 layer structure.[23] The $[Cu(moe)_2]$ compound, for which the structure has not been reported, is not very soluble, but soluble Cu alkoxides can be prepared using stronger donor-atoms in the ligands, as in the nitrogen-donor containing $[Cu(OC_2H_4NMe_2)_2]$,[24] or by adding more ether oxygen donors that can interact with the solvent or form more extensively chelated complexes.[25, 26] With higher metal-ion valencies, the methoxyethoxides are usually soluble, for exmple $[Gd_6O(MOE)_{16}]$, $[Y(MOE)_3]_{10}$, $[\{Bi(MOE)_3\}_\infty]$ and $[Pr_4O_2(MOE)_8]$.[27–30]

Here, we report the synthesis of $[Mn_{19}O_{12}(MOE)_{14}(MOEH)_{10}] \cdot MOEH$ from anhydrous $MnCl_2$ and potassium methoxyethoxide, and its solid-state structure determined from single-crystal X-ray data. Characterisation was performed by FTIR and UV/Vis spectroscopy, magnetic susceptometry, and differential scanning calorimetry.

Abstract in Swedish: *Alkoxider är av stort intresse som utgångsämnen för sol-gel-framställning av avancerade keramer, men det finns mycket lite av ens elementär kunskap om lågvalenta alkoxider av 3d-element. Den nya oxo-alkoxiden $[Mn_{19}O_{12}(MOE)_{14}(MOEH)_{10}] \cdot MOEH$ $(MOE = OC_2H_2O\text{-}CH_3)$ framställdes, genom metates och självnedbrytning, ur $MnCl_2$ och kalium metoxy-etoxid i toluen/MOEH, och kristallstrukturen bestämdes med enkristall-röntgendiffraktion: trigonal cell, rymdgrupp $R\bar{3}$ (no 148), $a = 27.560(3)$, $c = 19.294(2)$ Å, $Z = 3$, $R1 = 0.0737$, $wR2 = 0.1609$. De enskilda molekylerna har formen av platta skivor, med en lagerstruktur av CdI_2-typ, där alla Mn-atomer är divalenta med oktaedrisk koordination av syreatomer. Den centrala Mn-atomen koordinerar sex oxo-syren, den mellersta ringens sex Mn atomer två oxo-syren och fyra MOE(H) grupper, medan den perifiera ringens tolv Mn-atomer vardera koordinerar ett oxo-syre och fem MOE(H)-grupper. Studier med svepdifferentialkalorimetri (DSC) visade att den första förändringen sker med början vid ca 100 °C. Den magnetiska susceptibilitetskurvan visar att $\chi_M T$ kontinuerligt minskar med sjunkande temperatur under 150 K, vilket troligen beror på antiferromagnetisk växelverkan. FTIR- och UV/Vis-spektroskopi på fasta och upplösta prover visade att strukturen i fast tillstånd ändras åtminstone i viss utsträckning vid upplösning i toluen-MOEH.*

Results and Discussion

Synthesis: The preparation of a soluble Mn alkoxide was achieved by metathesis of potassium methoxyethoxide and $MnCl_2$ in toluene/MOEH. The same product, identified by IR spectroscopy, has also been obtained by ligand exchange from a mixture of KCl and the insoluble $Mn(OiPr)_2$ or $Mn(OEt)_2$ by adding an excess of MOEH. Often small amounts of K or K + Cl were present in the product, and therefore recrystallisation was necessary for a pure product to be obtained. Eliminating K and Cl impurities became much more difficult in the presence of even small amounts of Mn^{III}, and it was therefore crucial to prevent any oxidation during the preparation. This requires absolutely inert atmosphere and oxygen-free solvents, as the Mn^{II} ion is extremely susceptible to oxidation because of its highly basic ligands. The crystallisation of $[Mn_{19}O_{12}(moe)_{14}(moeH)_{10}] \cdot MOEH$ was rather slow, taking approximately two weeks or more, so that a decomposition of the alkoxide into the structurally determined oxo-alkoxide was suspected. However, the UV-Vis spectra of solutions obtained before and after work-up were quite similar (see Figure 3 below), showing that the same Mn compound was present before and after crystallisation, and thus an explanation for the slow crystallisation has to be sought elsewhere. Formation of unexpected oxo groups in alkoxides have been explained by hydrolysis from unintentionally added small amounts of water stemming from the solvents or precursors. In our case this seems unlikely, since we have used the same manganese source and solvent-drying procedures to prepare high yields of other alkoxides that do not contain oxo-ions, and, therefore, we believe that the oxo-alkoxide is formed immediately by decomposition of the organic ligands when the precursors react. $[Mn_{19}O_{12}(moe)_{14}(moeH)_{10}] \cdot MOEH$ is stable over time and is soluble in MOEH, toluene and *iso*-propanol, although partial ligand exchange cannot be excluded in the latter case. The solubility is very low in hexane.

Thermal studies: Inspection of crystals in the melting-point apparatus showed that liquid condensed in the cold part of the capillary at temperatures around 120–140 °C, but no melting or other changes could be observed until a temperature of about 200 °C was reached and the crystals darkened. Heating

0947-6539/01/0716-3440 $ 17.50+.50/0 *Chem. Eur. J.* **2001**, *7*, No. 16

the alkoxide at 5 °C min^{-1} in the differential scanning calorimetry (DSC) apparatus resulted in two endothermic peaks (Figure 1). The first peak, with an onset at 99–101 °C and a minimum at 107–109 °C (three separate runs), corresponds to an enthalpy of approximately 180 kJ mol^{-1}. On cooling after

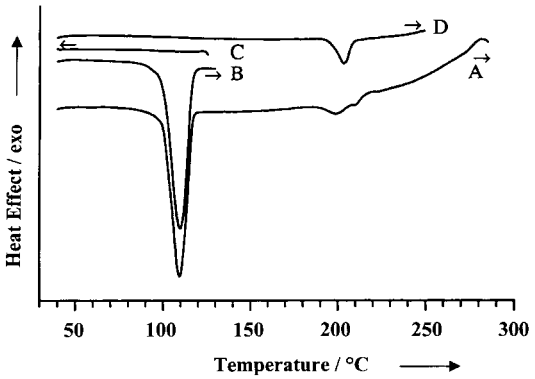

Figure 1. DSC runs obtained of $[Mn_{19}O_{12}(moe)_{14}(moeH)_{10}]\cdot MOEH$ at 5 °C min^{-1}; Sample 1: 20–270 °C (A), Sample 2: first heating 20–130 °C (B), then cooling 130–20 °C (C), and renewed heating 20–270 °C (D).

passing this endothermic peak at 130 °C, no peak due to recrystallisation was observed, as seen in Figure 1; neither was any endothermic peak observed on renewed heating from room temperature; this shows that the reaction is irreversible. This behaviour was also observed for $[Er_2Ti_4O_2(OEt)_{18}(HOEt)_2]$,[37] which irreversibly lost its two ethanol molecules at 102–106 °C with an enthalpy of -220 kJ mol^{-1}. In comparison, the melting enthalpy of alkoxides is normally smaller and reproducible, for example, about 20 kJ mol^{-1} for $[Er_5O(OiPr)_{13}]$.[38] Thus, the loss of liquid observed in this temperature range indicates that this endothermic peak is mainly due to loss of MOEH, and the size of the peak indicates that roughly one MOEH is lost. The fact that the endothermic peak starts at a temperature even lower than the boiling point of the MOEH (125 °C) might indicate that the interstitial MOEH molecule is lost in connection with melting, increased motion of the $[Mn_{19}O_{12}(moe)_{14}(moeH)_{10}]$ molecules, or some reaction. The IR spectrum of the faintly pink plastic material obtained from a DSC run to 130 °C showed changes both in the IR bands associated with the MOE(H) groups and in the Mn–O band, compared to the original alkoxide, indicating that major structural changes had occurred. The next endothermic peak had an onset at approximately 186 °C and a minimum at about 195 °C, corresponding to an enthalpy of ~20 kJ mol^{-1}; greyish-green spots, which indicated formation of MnO, were observed in the material quenched from this temperature.

Magnetic susceptibility studies: The $\chi_M T$ versus T curve of $[Mn_{19}O_{12}(moe)_{14}(moeH)_{10}]\cdot MOEH$ is shown in Figure 2. A constant $\chi_M T$ value of 56.1 cm^3 K mol^{-1} was observed above 200 K. Curie–Weiss behaviour is observed for the susceptibility in the temperature range 150 to 320 K. A linear least-squares fit gave $C = 55.5$ cm^3 K mol^{-1} and $\Theta = -4.15$ K ($R^2 = 0.9992$). The expected value of the Curie constant for 19 completely uncoupled Mn^{II} ions (with $g = 2.00$) is

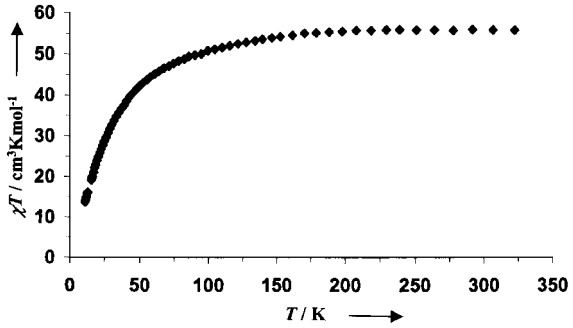

Figure 2. The $\chi_M T$ versus T curve of $[Mn_{19}O_{12}(moe)_{14}(moeH)_{10}]\cdot MOEH$.

83.12 cm^3 K mol^{-1}. The continuous decrease of μ_{eff} with decreasing temperature below 150 K may originate from antiferromagnetic interactions between the manganese centres within the molecule. However, these exchange interactions would probably give a nonzero-spin ground state of the molecule, since it contains an odd number of Mn^{II} ions arranged in an inner and outer ring structure.

UV/Vis and IR spectroscopy: The solid-state UV/Vis spectrum of the very faintly pink compound is shown in Figure 3. The peaks could be ascribed to electron transitions within the

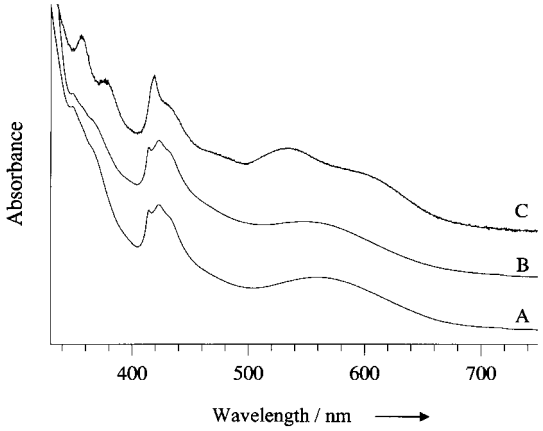

Figure 3. UV/Vis spectra of the synthesis solution 24 h after the mixing of the starting compounds and before the work-up (A); crystals dissolved in toluene/MOEH (2:3 vol/vol) solvent (B); crystals of $[Mn_{19}O_{12}(moe)_{14}(moeH)_{10}]\cdot MOEH$ (C).

d orbitals of octahedrally coordinated high-spin Mn^{II} ions:[39] ($^4T_{1g}(G) \leftarrow {}^6A_{1g}$ 18730 cm^{-1}, $^4T_{2g}(G) \leftarrow {}^6A_{1g}$ 21790 cm^{-1} (shoulder), $^4A_{1g}(G) \leftarrow {}^6A_{1g}$ and $^4E_g(G) \leftarrow {}^6A_{1g}$ 23470 (shoulder) and 23870 cm^{-1}, $^4T_{2g}(D) \leftarrow {}^6A_{1g}$ 26600 cm^{-1} and $^4T_g(D) \leftarrow {}^6A_{1g}$ 28120 cm^{-1}). These peaks fit well into the energies obtained for a ligand-field splitting (Δ_o) of 7500 cm^{-1} in the Orgel diagram provided by Lawrence et al.[40] The nephelauxetic parameters, B and C, were calculated according to the method described in reference [39] to be 620 and 3505 cm^{-1}, respectively. To fit the strong shoulder at 16950 cm^{-1} of the peak of lowest energy, the best fit in the Orgel diagram was obtained at a Δ_o value of about 9400 cm^{-1}. Whether the double-peak shape of the lowest-energy peak stems from different ligand fields at the different Mn atoms, from splitting due to the

  0947-6539/01/0716-3441 $ 17.50+.50/0

asymmetric coordination of the outer-ring Mn atoms, or from other effects, is not known at present.

The solution spectra obtained before and after work-up and after crystallisation were nearly identical, indicating that the solution structures are very similar, but somewhat different from that of the solid state. The peaks in the solution spectrum obtained by dissolution of the crystalline material in toluene/MOEH were assigned in the same way as for the solid alkoxide; $^4T_{1g}(G) \leftarrow {}^6A_{1g}$ 18180 cm^{-1}, $^4T_{2g}(G) \leftarrow {}^6A_{1g}$ 21600 cm^{-1} (shoulder), $^4A_{1g}(G) \leftarrow {}^6A_{1g}$ and $^4E_g(G) \leftarrow {}^6A_{1g}$ 23260 (shoulder), 23650 and 24140 cm^{-1}, $^4T_{2g}(D) \leftarrow {}^6A_{1g}$ 27530 cm^{-1} and $^4T_g(D) \leftarrow {}^6A_{1g}$ 28740 cm^{-1}. The peaks were fitted to the Orgel diagram at a Δ_o value of about 8500 cm^{-1}, and the *B* and *C* parameters were determined to be 690 and 3400 cm^{-1}, respectively. The ligand field in the solution is between the higher and lower fields that were observed for the solid state, but the peak at the lowest energy, which is the most sensitive to the ligand field, is quite broad and might be composed of several peaks with a wide spread.

The ligand-field splitting in $[Mn_{19}O_{12}(moe)_{14}(moeH)_{10}]\cdot$MOEH is comparable to that observed for $[Mn(H_2O)_6]^{2+}$ in water (8500 cm^{-1}),[40] but clearly higher than the values of 5260 – 7710 cm^{-1} reported by Horvath et al. for manganese(II) alkoxides with methoxo, ethoxo, *iso*-propoxo and *tert*-butoxo ligands.[24]

From the IR spectra presented in Figure 4, and also the UV/Vis spectra, it is apparent that the structure changes to some extent when $[Mn_{19}O_{12}(moeH)_{14}(moeH)_{10}]\cdot$MOEH is dissolved. Virtually all peaks of the solid-state spectrum appear

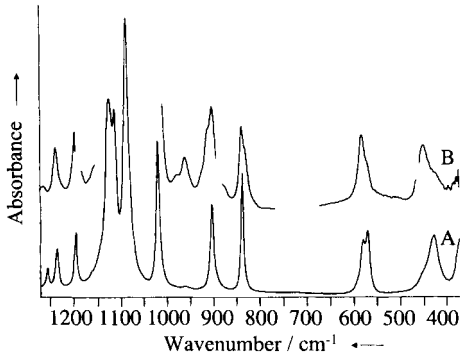

Figure 4. FTIR spectra of: $[Mn_{19}O_{12}(moe)_{14}(moeH)_{10}]\cdot$MOEH as solid crystals (A), dissolved in toluene/MOEH/hexane (1:2:3 vol:vol:vol) solvent (B). Parts of the graph have been deleted where the spectrum is unreliable because solvent absorption is too strong to be corrected for.

in approximately the same place in the solution spectrum, but are split or changed in intensity. Peaks of the solid-state spectrum in the C–O, C–C and Mn–O regions were found at: 1125, 1114, 1088, 1020, 903, 838, 580, 570, 428 and 370 cm^{-1}, while peaks of the solution spectrum were found at: 979, 962, 927 (sh), 912 (sh), 904, 839, 832 (sh), 583, 627 (sh), 452, 424 cm^{-1} (sh). In the solution spectrum, a broad absorption peak ascribed to O–H stretching of the solvating groups was observed, with a maximum at 3230 cm^{-1} well separated from the O–H stretch peak of the MOEH solvent at 3410 cm^{-1}; this indicates rather weak hydrogen bonds in the alkoxide-bonded MOE(H) groups.

But although there are some small changes in the UV/Vis and IR spectra when the alkoxide is dissolved, which indicates some change in the structure, it is probable that the structure in solution is rather similar to that of the solid state. Chemically, a disproportionation is also difficult to imagine, owing to the large number of oxo-bridges stretching throughout the molecule that should be very difficult to break up. The formation of two Mn alkoxides, one more and one less rich in oxo oxygen atoms, should be less likely because the number of oxo oxygens atoms is so high that this would most probably lead to precipitation of MnO, which is not observed.

The solid-state structure: The structure of $[Mn_{19}O_{12}(moe)_{14}(moeH)_{10}]\cdot$MOEH in the solid state was determined by single-crystal X-ray crystallography, and the molecular structure is shown in Figure 5. Selected bond lengths and angles are

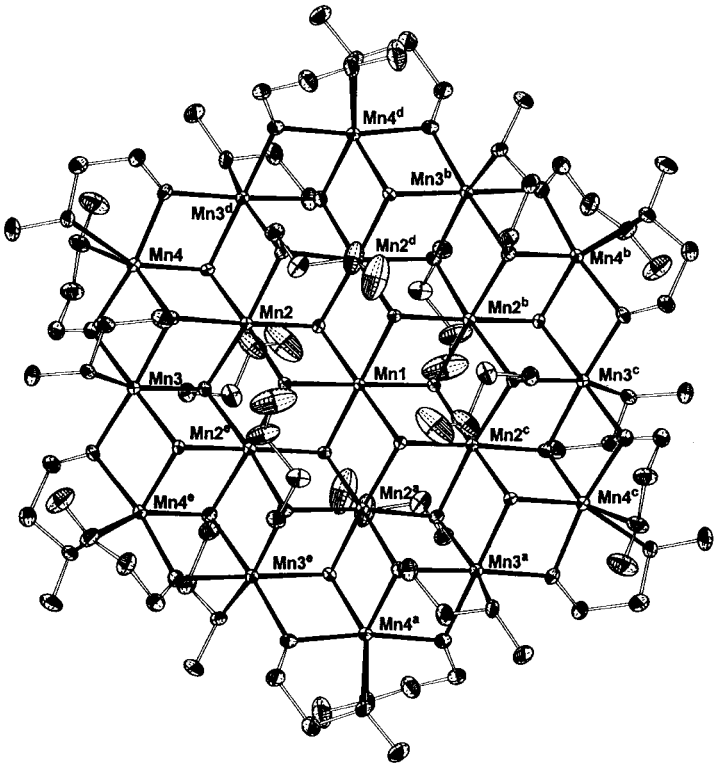

Figure 5. ORTEP (ellipsoids at 50% probability level) view of $[Mn_{19}O_{12}(moe)_{14}(moeH)_{10}]\cdot$MOEH.

given in Table 1. The unit cell contains three formula units of the disc-like Mn_{19} complex together with three MOEH molecules. The $M_{19}O_{54}$ core of the molecule is encapsulated by an organic shell built up of MOE and MOEH. The C–O bond lengths in these ligands are in the range 1.393(8) – 1.444(9) Å. The Mn_{19} complex consists of four crystallographically independent Mn atoms that are connected to each other through oxo oxygen atoms or MOE(H) oxygen atoms. The central Mn1 atom, which has $\bar{3}$ symmetry (Wyckoff position 3a), is coordinated by six μ_3-oxo atoms that are also connected to an outer ring consisting of six Mn2 atoms. These Mn2 atoms, in turn, are connected to an additional peripheral ring consisting of a total of twelve alternating Mn3 and Mn4 atoms.

0947-6539/01/0716-3442 $ 17.50+.50/0 *Chem. Eur. J.* **2001**, *7*, No. 16

Table 1. Selected bond lengths [Å] and angles [°] for $[Mn_{19}O_{12}(moe)_{14}(moeH)_{10}]\cdot MOEH$.[a]

Mn1–O1	2.193(3)	Mn3–O6	2.118(4)
Mn2–O1	2.134(4)	Mn3–O3^e	2.199(2)
Mn2–O1^c	2.182(2)	Mn3–O2	2.201(3)
Mn2–O3	2.185(4)	Mn3–O4	2.243(5)
Mn2–O4	2.203(3)	Mn3–O8	2.309(4)
Mn2–O2^c	2.213(3)	Mn4–O6^e	2.072(2)
Mn2–O2	2.255(4)	Mn4–O5	2.080(4)
Mn3–O5	2.079(5)	Mn4–O3^e	2.136(4)
Mn3–O6	2.118(4)	Mn4–O4^e	2.199(3)
Mn3–O3^e	2.199(2)	Mn4–O9	2.385(4)
Mn3–O2	2.201(3)	Mn4–O7	2.404(4)
Mn3–O4	2.243(5)		
O1-Mn1-O1^a	99.02(10)	O4-Mn2-O2	82.99(13)
O1-Mn1-O1^d	99.02(13)	O4-Mn2-O2^c	96.63(10)
O1-Mn1-O1^b	179.99(12)	O4-Mn3-O8	75.24(13)
O1-Mn1-O1^c	80.98(10)	O4^e-Mn4-O7	154.44(13)
O1-Mn2-O1^c	82.59(10)	O4^e-Mn4-O9	107.70(13)
O1-Mn2-O2^c	105.40(13)	O5-Mn3-O2	105.18(14)
O1-Mn2-O2	82.79(14)	O5-Mn3-O3^e	78.12(15)
O1^c-Mn2-O2^c	82.71(3)	O5-Mn3-O4	171.01(15)
O1^c-Mn2-O2	97.16(9)	O5-Mn3-O6	102.23(17)
O1-Mn2-O3	171.14(16)	O5-Mn3-O8	95.81(15)
O1^c-Mn2-O3	93.25(10)	O5-Mn4-O3^e	79.54(13)
O1-Mn2-O4	100.91(15)	O5-Mn4-O4^e	105.88(12)
O1^c-Mn2-O4	176.48(10)	O5-Mn4-O7	99.59(15)
O2^c-Mn2-O2	171.68(10)	O5-Mn4-O9	74.02(15)
O2-Mn3-O4	83.32(13)	O6-Mn3-O2	98.81(15)
O2-Mn3-O8	154.75(13)	O6-Mn3-O3^e	179.29(14)
O3-Mn2-O2^c	81.71(11)	O6-Mn3-O4	78.94(16)
O3-Mn2-O2	90.00(14)	O6-Mn3-O8	90.11(15)
O3-Mn2-O4	83.23(14)	O6^e-Mn4-O3^e	108.32(10)
O3^e-Mn3-O2	81.66(13)	O6^e-Mn4-O4^e	80.95(11)
O3^e-Mn3-O4	100.61(13)	O6^e-Mn4-O5	170.31(15)
O3^e-Mn3-O8	89.25(14)	O6^e-Mn4-O7	74.05(14)
O3^e-Mn4-O4^e	84.47(12)	O6^e-Mn4-O9	97.52(15)
O3^e-Mn4-O7	98.26(14)	O9-Mn4-O7	81.16(13)
O3^e-Mn4-O9	153.02(13)		
Mn2-O1-Mn2^e	99.44(17)	Mn3-O2-Mn2	96.37(13)
Mn2-O1-Mn1	98.83(15)	Mn3-O5-Mn4	103.34(21)
Mn2^e-O1-Mn1	97.37(13)	Mn4^e-O3-Mn2	97.31(16)
Mn2^e-O2-Mn2	94.93(16)	Mn4^e-O3-Mn3^e	97.60(14)
Mn2-O3-Mn3^e	98.76(18)	Mn4^e-O4-Mn2	94.96(16)
Mn2-O4-Mn3	96.67(14)	Mn4^e-O4-Mn3	95.00(17)
Mn3-O2-Mn2^e	97.88(15)	Mn4^e-O6-Mn3	102.81(20)

[a] Symmetry codes: a: $-y, x-y, z$; b: $-x, -y, -z$; c: $y, -x+y, -z$; d: $-x+y, -x, z$; e: $x-y, x, -z$.

The oxygen bridges between the Mn2 atoms and the peripheral Mn3 and Mn4 atoms are alternately μ_3-oxo atoms and μ_3-O-$C_2H_4OCH_3$ oxygen atoms.

The geometrical distortions exhibited at the outer Mn3 and Mn4 atoms are very pronounced in comparison to the comparatively regular MnO_6 coordination sphere of the Mn1 and Mn2 atoms (Figure 6). These distortions were analysed by a method that uses root harmonic mean squares for estimating the effective shapes and sizes of Jahn–Teller active ions such as Mn^{III} in oxides and fluorides.[41] As a result, although the coordination octahedra of Mn3 and Mn4 are severely distorted, these atoms should not be considered as trivalent ions. In order to further assess the divalent oxidation state of the Mn atoms from the X-ray diffraction structural parameters, bond valence sums (bvs) were calculated and are given in Table 2. These calculations were performed for the

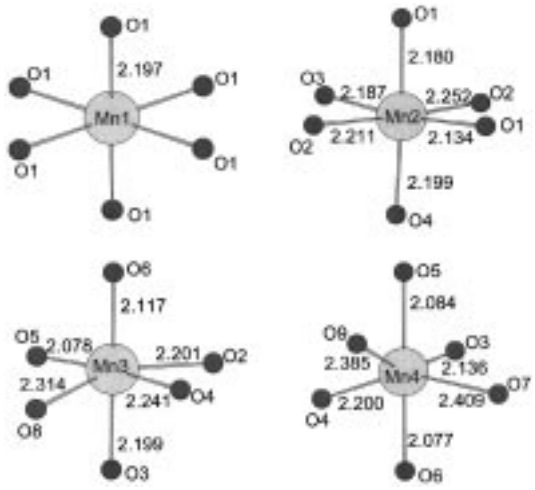

Figure 6. Comparison of the MnO_6 coordination geometries for Mn1, Mn2, Mn3 and Mn4.

Table 2. Bond valence analysis for the different Mn atoms in $[Mn_{19}O_{12}(moe)_{14}(moeH)_{10}]\cdot MOEH$.

Atom	Assumed oxidation state	
	Mn^{II}	Mn^{III}
Mn1	1.997	1.842
Mn2	2.023	1.865
Mn3	2.070	1.909
Mn4	2.024	1.866

two possible oxidation states, Mn^{II} and Mn^{III}. The bond valence analysis was based on the method by Brese and O'Keeffe.[42, 43] The result of the bvs analysis, namely divalent oxidation state for all the manganese atoms, is in accordance with the magnetic and spectroscopic measurements.

The title complex exhibits a metal-oxygen structure very much like a fragment of the brucite-group $Mn(OH)_2$ pyrochroite mineral.[44] This similarity holds also for some of the geometrical parameters such as bond lengths. The Mn–O bond lengths in the pyrochroite mineral and those of Mn1–O1 in the complex are identical within one standard deviation. The Mn–Mn distances in the complex are in the range of 3.242(2)–3.327(2) Å and compare well with the Mn–Mn separation of 3.32 Å in the mineral. In addition, the metal–metal distances in $[Mn_{19}O_{12}(moe)_{14}(moeH)_{10}]\cdot MOEH$ are in agreement with the Mn^{II}–Mn^{II} distances reported for other divalent Mn complexes, such as Mn_2^{II} dimers.[45]

The inner "$Mn1Mn2_6$" core of $[Mn_{19}O_{12}(moe)_{14}(moeH)_{10}]\cdot MOEH$ is similar to the previously described Anderson structure,[46] which consists of a central, octahedrally coordinated metal atom surrounded by six additional MO_6 octahedra. A few other manganese-containing Anderson-type molecules have been reported to date, and of particular interest are two molecular magnets, the mixed-valence heptanuclear alkoxo manganese cluster $[Mn_7(OMe)_{12}(dbm)_6]\cdot CHCl_3\cdot 14\,MeOH$[47] and the ferromagnetic cluster $[NaMn_6(OMe)_{12}(dbm)_6]BPh_4\cdot 2\,CHCl_3$,[48] in which the central Mn atom has been replaced by a non-magnetic alkali-metal ion.

Although no polynuclear manganese Mn_{19} cluster has been reported to date, a cationic hydroxo(oxo)iron cluster exists, with the composition $[Fe_{19}(\mu_3\text{-}O)_6(\mu_3\text{-}OH)_6(\mu_2\text{-}OH)_8(heidi)_{10}(H_2O)_{12}]^+$ ($H_3heidi = N(CH_2COOH)_2(CH_2CH_2OH)$),[49] in which the 19 Fe atoms arranged in a planar fashion. This complex also has a cluster core whose geometry is related to the AB_2 structural type found in, for example, $Mn(OH)_2$.

Conclusion

A novel disclike molecule, $[Mn_{19}O_{12}(moe)_{14}(moeH)_{10}]\cdot MOEH$, has been prepared by metathesis from $MnCl_2$ and potassium methoxyethoxide, and its solid-state structure has been determined by single-crystal X-ray diffraction. It is one of the largest alkoxide molecules as well as one of very few Mn alkoxides reported. All Mn atoms are divalent, and there are magnetic exchange interactions between the spins of the Mn atoms so that the molecule could have interesting magnetic properties that are of importance in the field of molecular magnetism. A collaboration on a more detailed study on the magnetic properties is presently being conducted. The solubility and reactivity, together with the layer structure make it a very good precursor for Mn-containing ceramics based on MnO_x layers, for example, perovskites such as $Ca_{0.33}La_{0.67}MnO_3$ in which the Mn-oxide layers alternate with $Ca_{0.33}La_{0.67}$-oxide layers, and sol-gel syntheses with this precursor are undertaken presently.

Experimental Section

Chemicals and equipment: All reactions, mixing of solutions and preparation of samples for analysis were carried out in a glove-box with dry, oxygen-free Ar atmosphere (Mecaplex GB80 or Braun MB200). The solvents were dried by distillation over CaH_2 under N_2 atmosphere. The anhydrous $MnCl_2$ (Merck p.a.) and K (Acros 98 + %) were used as purchased.

The IR studies were performed with a Bruker IFS-55 FT spectrometer in the range 360 – 5000 cm^{-1} on samples prepared as paraffin mulls between KBr discs and solutions in a closed KBr cell of 0.1 mm path length. The UV/Vis/NIR spectra were recorded with a Perkin – Elmer Lambda 19 dispersive spectrometer in the range 250 – 1000 nm for liquids or solids in quartz cells, in the case of the solid-state studies equipped with a 60 mm reflectance sphere using a transmission mode. A Jeol 820 scanning electron microscope equipped with a Link 10000AN energy-dispersive X-ray spectrometer (SEM-EDS) was used for determination of the K, Cl, and Mn contents in crystals or solutions that had been air-hydrolysed and dried. The detection limit is about 0.3 mol%. The thermal stability was investigated by differential scanning calorimetry (DSC) with a Perkin – Elmer Pyris 1 instrument, by using crystals in sealed steel capsules, and by ocular studies in sealed glass capillaries, with a Gallenkamp melting-point apparatus. The temperature and enthalpy were calibrated with standards of In, Pb, and bensoic acid. The in-phase component AC magnetic susceptibility of polycrystalline $[Mn_{19}O_{12}(moe)_{14}(moeH)_{10}]\cdot MOEH$ was measured (500 Hz and 125 $A\,m^{-1}$) on a sample in an air-tight teflon container, in the temperature range 11 – 320 K by using a Lake Shore AC Susceptometer, Model 7130, equipped with a helium cryostat. Diamagnetic corrections were made using Pascal's constants.[31]

Crystal structure determination: Single-crystal X-ray data for $[Mn_{19}O_{12}(moe)_{14}(moeH)_{10}]\cdot MOEH$ were collected on a STOE-IPDS image-plate diffractometer at $T = 110$ K and were corrected for Lorentz, polarisation and absorption effects by using the X-shape program package.[32] Additional crystallographic data are given in Table 3. The structure was solved by direct methods (SHELXS97)[33] and refined by full-matrix least-squares on F^2 (SHELXL97).[34, 35] The anionic MOE groups and the solvate MOEH molecules could not be distinguished from each other, due to the relatively poor quality of the diffraction data. Highly disordered MOEH molecules with partial occupancy factors for the C and O atoms were located in the Mn_{19} intermolecular voids. The structure was analysed by the SQUEEZE option of PLATON[36] in order to find further disordered solvent molecules. However, the residual void electron density in the three possible cavities did not give any chemically reasonable MOEH molecular geometries. The total electron count per cavity was 73 e^-, a number which approximately corresponds to two MOEH molecules. This indicates that the cavities between the Mn_{19} molecules are partially filled with very diffusely positioned solvent molecules. Moreover, since the data were collected at low temperature, it is likely that the MOEH molecules are statistically disordered. The R values are defined as: $R(\mathrm{int}) = \Sigma|F_o^2 - F_o^2(\mathrm{mean})|/\Sigma[F_o^2]$, $S = [\Sigma[w(F_o^2 - F_c^2)^2]/(n-p)]^{1/2}$, $R1 = \Sigma||F_o| - |F_c||/\Sigma|F_o|$, $wR2 = [\Sigma[w(F_o^2 - F_c^2)^2]/\Sigma[w(F_o^2)^2]]^{1/2}$.

Table 3. Selected crystal data for $[Mn_{19}O_{12}(moe)_{14}(moeH)_{10}]\cdot MOEH$.

empirical formula	$C_{72}H_{178}Mn_{19}O_{60}C_3H_8O_2$
M_r	3124.12
crystal system	trigonal
space group	$R\bar{3}$ (No. 148)
a [Å]	27.560(3)
c [Å]	19.294(2)
V [Å$_3$]	12691(2)
Z	3
crystal size (mm^3)	$0.09 \times 0.34 \times 0.42$
ρ_{calcd} [$g\,cm^{-3}$]	1.226(1)
T [K]	110(1)
μ ($Mo_{K\alpha}$) [mm^{-1}]	1.43
$F(000)$	960.0
reflections observed	2948
parameters	240
R(int)	0.163
S(goodness of fit)	0.909
$R1/wR2$, $[I > 2\sigma(I)]$	0.0737/0.1609
$\Delta\rho_{max}/\Delta\rho_{min}$ [$e\,Å^{-3}$]	0.867/ – 0.584

Synthesis: Elemental K (1.000 g, 25.58 mmol) was dissolved in MOEH or MOEH/toluene (2:1 vol/vol; 25 mL), whereupon $MnCl_2$ (1.610g, 12.79 mmol) was added under stirring. After 24 hours, the mixture was centrifuged to separate the white KCl formed, and the pale pink solution part was evaporated; this resulted in the formation of a husk of crystals on the vessel walls. Frequently, the obtained Mn alkoxide contained small amounts of K or K + Cl, according to the SEM-EDS analyses. After redissolution in toluene/MOEH and centrifugation, a crystal husk on the vessel walls was slowly formed on evaporation of the solvent, which contained no detectable K or Cl. The crystals used for X-ray analysis were cut out from such a husk and cleaned. Yield: typically 85%.

Acknowledgements

Financing of this work by the Swedish Natural Science Research Council, NFR, is gratefully acknowledged. We also wish to thank Dr. K. Jansson and E. Wikstad for aid in the DSC measurements.

[1] M. McCormack, S. Jin, T. H. Tiefel, R. M. Fleming, J. M. Phillips, R. Ramesh, *Appl. Phys. Lett.* **1994**, *64*, 3045.
[2] R. Mahendiran, R. Mahesh, A. K. Raychaudhuri, C. N. R. Rao, *Phys. Rev. B* **1996**, *53*, 12160.
[3] L. Righi, P. Gorria, M. Insausti, J. Gutiérrez, J. M. Barandiarán, *J. Appl. Phys.* **1997**, *81*, 5767.
[4] N. Zhang, W. Ding, W. Zhong, D. Xing, Y. Du, *J. Mater. Sci.* **1999**, *34*, 1829.

0947-6539/01/0716-3444 $ 17.50+.50/0 *Chem. Eur. J.* **2001**, *7*, No. 16

[5] A. M. Balbashov, S. G. Karabashev, Y. M. Mukovskiy, S. A. Zverkov, *J. Cryst. Growth* **1996**, *167*, 365.
[6] Y. Shimakawa, Y. Kubo, T. Manako, *Nature* **1996**, *379*, 53.
[7] M. A. Subramanian, B. H. Toby, A. P. Ramirez, W. J. Marshall, A. W. Sleight, G. H. Kwei, *Science* **1996**, *273*, 81.
[8] P. Artizzu-Duart, Y. Brullé, F. Gaillard, E. Garbowski, N. Guilhaume, M. Primet, C*atal. Today* **1999**, *54*, 181.
[9] K. S. Yooa, N. W. Chob, Y.-J. Oh, *Solid State Ionics* **1998**, *113 – 115*, 43.
[10] N. Fujimura, T. Ishida, T. Yoshimura, T. Ito, *Appl. Phys. Lett.* **1996**, *69(7)*, 1011.
[11] N. Fujimura, S. Azuma, N. Aoki, T. Yoshimura, *Appl. Phys. Lett.* **1996**, *80(12)*, 7084.
[12] N. Aoki, N. Fujimura, T. Yoshimura, T. Ito, *J. Cryst. Growth* **1997**, *174*, 796.
[13] T. Yoshimura, N. Fujimura, N. Aoki, K. Hokayama, S. Tsukui, K. Kawabata, T. Ito, *Jpn. Appl. Phys.* **1997**, *36*, 5921.
[14] T. Nomura, K. Okutani, T. Ochai in *Advanced Ceramics* (Ed.: S. Saito), Oxford Science, **1988**, pp. 254.
[15] R. W. Adams, E. Bishop, R. L. Martin, G. Winter, *Aust. J. Chem.* **1966**, *19*, 207.
[16] B. Horvath, R. Möseler, E. G. Horvath, *Z. Anorg. Allg. Chem.* **1979**, *449*, 41.
[17] B. D. Murray, H. Hope, P. P. Power, *J. Am. Chem. Soc.* **1985**, *107*, 169.
[18] M. Veith, D. Käfer, J. Koch, P. May, L. Stahl, V. Huch, *Berichte* **1992**, *125*, 1033.
[19] G. Westin, *J. Sol Gel Sci. Technol.* **1988**, *12*, 203.
[20] U. Bemm, R. Norrestam, M. Nygren, G. Westin, *J. Solid State Chem.* **1997**, *134*, 312.
[21] U. Bemm, R. Norrestam, M. Nygren, Westin, *Inorg. Chem.* **1995**, *34*, 2367.
[22] S. C. Goel, M. Y. Chiang, W. E. Buhro, *Inorg. Chem.* **1990**, *29*, 4640.
[23] S. C. Goel, M. A. Matchett, M. Y. Chiang, W. E. Buhro, *J. Am. Chem. Soc.* **1991**, *113*, 1844.
[24] S. C. Goel, K. S. Kramer, M. Y. Chiang, W. E. Buhro, *Polyhedron* **1990**, *9*, 611.
[25] G. Westin, unpublished results.
[26] H. S. Horowitz, S. J. McLain, A. W. Sleight, J. D. Druliner, P. L. Gai, M. J. VanKavelaar, J. L. Wagner, B. D. Viggs, S. J. Poon, *Science* **1989**, *243*, 66.
[27] S. Daniele, L. G. Hubert- Pfalzgraf, J.-C. Daran, *Polyhedron* **1996**, *15*, 1063.
[28] O. Poncelet, L. G. Hubert-Pfalzgraf, J.-C. Daran, R. Astier, *J. Chem. Soc. Chem. Commun.* **1989**, 1846.
[29] M. A. Matchett, M. Y. Chiang, W. E. Buhro, *Inorg. Chem.* **1990**, *29*, 358.
[30] L. G. Hubert- Pfalzgraf, S. Daniele, A. Bennaceur, J.-C. Daran, J. Vaissermann, *Polyhedron* **1997**, *16*, 1223.
[31] E. A. Boudreaux, L. N. Mulay, *Theory and Applications of Molecular Paramagnetism*, Wiley, New York, **1976**.
[32] STOE, *X-SHAPE*, *revision 1.09*, *Crystal Optimisation For Numerical Absorption Correction*, Darmstadt (Germany), **1997**.
[33] G. M. Sheldrick, *SHELXL97 Program for the Refinement of Crystal Structures*, University of Göttingen (Germany), **1997**.
[34] G. M. Sheldrick, *Acta Crystallogr. Sect. A* **1990**, *46*, 467.
[35] Crystallographic data (excluding structure factors) for the structures reported in this paper have been deposited with the Cambridge Crystallographic Data Centre as supplementary publication no. CCDC-149155. Copies of the data can be obtained free of charge on application to CCDC, 12 Union Road, Cambridge CB2 1EZ, UK (fax: (+44) 1223-336-033; e-mail: deposit@ccdc.cam.ac.uk).
[36] A. L. Spek, *PLATON*, *A Multipurpose Crystallographic Tool*, Utrecht University, Utrecht (The Netherlands) **2000**.
[37] G. Westin, M. Kritikos, M. Wijk, *J. Solid State Chem.* **1998**, *141*, 168.
[38] G. Westin, R. Norrestam, M. Nygren, M. Wijk, *J. Solid State Chem.* **1998**, *135*, 149.
[39] *Inorganic Electronic Spectroscopy*, 2nd ed., Elsevier, Amsterdam, **1984**, p. 448.
[40] L. J. Heidt, G. F. Koster, A. M. Johnson, *J. Am. Chem. Soc.* **1959**, *81*, 6471.
[41] R. Norrestam, *Z. Kristallog.* **1994**, *209*, 99.
[42] N. E. Brese, M. O'Keeffe, *Acta Crystallogr. Sect. B* **1991**, *47*, 192.
[43] I. D. Brown, D. Altermatt, *Acta Crystallogr Sect. B.* **1985**, *41*, 244.
[44] A. Noerlund-Christensen, G. Ollivier, *Solid State Commun.* **1972**, *10*, 609.
[45] N. A. Law, M. T. Caudle, V. L. Pecoraro, *Adv. Inorg. Chem.* **1999**, *46*, 305.
[46] L. C. W. Baker, D. C. Glick, *Chem. Rev.* **1998**, *98*, 3 and references therein.
[47] G. L Abbati, A. Cornia, A. C. Fabretti, A. Caneschi, D. Gatteschi, *Inorg. Chem.* **1998**, *37*, 3759.
[48] G. L. Abbati, A. Cornia, A. C. Fabretti, A. Caneschi, D. Gatteschi, *Inorg. Chem.* **1998**, *37*, 1430.
[49] S. L. Heath, A. K. Powell, *Angew. Chem.* **1992**, *104*, 191; *Angew. Chem. Int. Ed. Engl.* **1992**, *31*, 191.

Received: September 11, 2000
Revised: March 9, 2001 [F2722]